

ELECTRONIC SUPPORTING INFORMATION

Direct observation of conformational changes of adipate dianions encapsulated in water clusters

Geng-Geng Luo,^{*a} Dong-Liang Wu,^a Ji-Huai Wu,^a Jiu-Xu Xia,^a Li Liu,^a Jing-Cao Dai^a

Institute of Materials Physical Chemistry, College of Materials Science & Engineering, Huaqiao University, Xiamen 361021, China

Electronic Supporting Information

Materials and general methods.....	S2
Synthesis of 1-2.....	S2
X-ray crystallography	S3
Table S1. Crystal data and structure refinement for 1-2.....	S4
Table S2. Atomic coordinates and equivalent isotropic displacement parameters (\AA^2) for 1-2	S5
Table S3. Bond distances (\AA) and angles ($^\circ$) for 3.....	S7
Table S4. Relevant Hydrogen-bonding parameters in 1 and 2.....	S8
Figure S1. FT-IR spectra of 1-2.....	S9
Figure S2. TGA curves of 1-2.....	S10
Figure S3. PXRD patterns and the simulated ones from the single-crystal diffraction data for 1-2	S12
Figure S4. ORTEP diagrams showing the building units of crystal structures in 1-2.....	S13
Figure S5. 2D water-adip anionic layer formed by hydrogen-bonding in 1.....	S14
Figure S6. 2D water-adip anionic layer formed by hydrogen-bonding in 2.....	S15
Figure S7. Metallo-supramolecular sandwich lamellar networks occurred in 1-2.....	S16

Materials and general methods

All reagents and solvents for synthesis were purchased from commercial sources and used as received. The C, H and N microanalyses were carried out with a CE instruments EA 1110 analyzer. The FT-IR spectra were recorded from KBr pellets in the range of 4000–400 cm⁻¹ on a Nicolet Nexus 470 spectrometer. TG curves were performed from 25 to 800 °C on a TA5200/MDSC2910 instrument at a heating rate of 5 °C·min⁻¹. Powder X-ray diffraction (PXRD) patterns were recorded on well-ground samples in the 2θ range of 5–50° using a Bruker AXS D8-Advanced diffractometer at 40 kV, 40 mA with Cu Kα radiation with a scan speed of 5°·min⁻¹ and a step size of 0.1° in 2θ.

Synthesis of 1-2

Synthesis of {[Ag₂(bpe)₂(H₂O)₂](adip)}·6H₂O} (1). A mixture of Ag₂O (115 mg, 0.5 mmol), bpe (193 mg, 1 mmol) and H₂adip (146 mg, 1 mmol) was treated in CH₃OH-H₂O mixed solvent (10 ml, v/v: 1:1) under ultrasonic treatment (160 W, 40 kHz) at ambient temperature for 10 min. Then, an aqueous NH₃ solution (25%) was dropped into the mixture to give a clear solution. The resultant solution was allowed to evaporate slowly in darkness at room temperature for several days to give colorless crystals of **1** (yield 47%, based on Ag₂O). They were washed with a small volume of cold CH₃OH and diethyl ether. Anal. Calcd (%) for C₁₅H₂₄AgN₂O₆: C 41.30, H 5.55, N 6.42; found: C 41.40, H 5.61, N 6.48. FT-IR (KBr, cm⁻¹): ν = 3430(s), 3030(w), 2933(w), 2864(w), 1608(s), 1563(s), 1416(s), 1320(w), 1218(m), 1077(m), 1014(m), 992(m), 918(w), 828(m), 550(w).

Synthesis of {[Ag(bpp)(H₂O)·Ag(bpp)](adip)}·9H₂O} (2). The reaction was carried out in a method similar to that for **1**, using bpp (205 mg, 1 mmol) instead of bpe ligand. Colorless crystals of **2** were obtained in 59% yield based on Ag₂O. They were washed with a small volume of cold CH₃OH and diethyl ether. Anal. Calcd (%) for C₃₂H₅₆Ag₂N₄O₁₄: C 41.04, H 6.03, N 5.98; found: C 40.96, H 6.08, N 5.94. FT-IR (KBr, cm⁻¹): ν = 3460(s), 3244(br), 3028(w), 2950(w), 1612(s), 1558(s), 1420(s), 1300(m), 1222(m), 1078(m), 1018(m), 832(s), 677(m), 551(m).

X-ray crystallography

Single crystals of complexes **1** and **2** with appropriate dimensions were selected under an optical microscope and quickly coated with high vacuum grease (Dow Corning Corporation) before being mounted on a glass fiber for data collection. Data were collected at 173(2) K on a Rigaku R-AXIS RAPID Image Plate single-crystal diffractometer with graphite-monochromated Mo K α radiation source ($\lambda = 0.71073 \text{ \AA}$) operating at 50 kV and 90 mA in ω scan mode for **1-2**. A total of $44 \times 5.00^\circ$ oscillation images was collected, each being exposed for 5.0 min. Absorption correction was applied by correction of symmetry-equivalent reflections using the ABSCOR program.¹ In both cases, the highest possible space group was chosen. All the structures were solved by direct methods using SHELXS-97² and refined on F^2 by full-matrix least-squares procedures with SHELXL-97.³ Atoms were located from iterative examination of difference F -maps following least squares refinements of the earlier models. Hydrogen atoms on organic ligands were placed in calculated positions and included as riding atoms with isotropic displacement parameters 1.2-1.5 times U_{eq} of the attached C atoms. The water H atoms in **1-2** were located in difference Fourier maps, their bond lengths were set to ideal values and finally they were refined using a riding model with O-H = 0.80 \AA . C4 atom for complex **2** is restrained by ISOR. Moreover, one of the silver ions (Ag3) in the asymmetric unit of complex **2** is disordered about the crystallographic center of inversion. All the structures were examined using the Addsym subroutine PLATON⁴ to assure that no additional symmetry could be applied to the models. Crystal structure views were obtained using Diamond v3.1f.⁵ Hydrogen bonding interactions in the crystal lattices **1-2** were calculated by PLATON.⁴

References

- (1) T. Higashi, ABSCOR, Empirical Absorption Correction based on Fourier Series Approximation, Rigaku Corporation, Tokyo, 1995.
- (2) G. M. Sheldrick, SHELXS-97, Program for X-ray Crystal Structure Determination, University of Göttingen, Germany, 1997.
- (3) G. M. Sheldrick, SHELXL-97, Program for X-ray Crystal Structure Refinement, University of Göttingen, Germany, 1997.
- (4) PLATON, A. L. Spek, *Acta Cryst.* 1990, **A46**, C-34.
- (5) Brandenburg, K. DIAMOND, version 3.1f, Crystal Impact GbR, Bonn, Germany, 2008.

Table S1. Crystal data and structure refinement for **1-2**.

Complex	1(CCDC 837533)	2(CCDC 837534)
Empirical formula	C ₁₅ H ₂₄ AgN ₂ O ₆	C ₃₂ H ₅₆ Ag ₂ N ₄ O ₁₄
Temperature	173(2)K	173(2)K
Formula weight	436.23	936.55
Crystal system	Monoclinic	Orthorhombic
Space group	<i>P</i> 2 ₁ /c	<i>P</i> bca
<i>a</i> (Å)	11.134(2)	8.996(2)
<i>b</i> (Å)	16.751(3)	25.246(5)
<i>c</i> (Å)	9.859(2)	35.100(7)
β (°)	106.73(3)	90
Z, <i>D</i> _{calc} (Mg/m ³)	4, 1.646	8, 1.561
<i>V</i> (Å ³)	1760.8(6)	7972(3)
μ(mm ⁻¹)	1.18	1.05
<i>F</i> (000)	892	3856
Total no. of reflns.	11422	29708
No. of unique reflns.	3052 (<i>R</i> _{int} = 0.033)	6771 (<i>R</i> _{int} = 0.079)
No. of variables	2613	4308
Parameters	217	475
Final R indices [I > 2σ(I)]	R ₁ = 0.0271, wR ₂ = 0.0820	R ₁ = 0.0701, wR ₂ = 0.1878
R indices (all data)	R ₁ = 0.0339, wR ₂ = 0.0941	R ₁ = 0.1137, wR ₂ = 0.2159
Goodness-of-fit on F ²	1.127	1.04
Largest diff. peak and hole (e Å ⁻³)	0.48 and -0.48	1.14 and -1.02

$$^aR_1 = \Sigma |F_o| - |F_c| / \Sigma |F_o|, ^b wR_2 = [\Sigma w(F_o^2 - F_c^2)^2] / \Sigma w(F_o^2)^2]^{1/2}$$

Table S2. Atomic coordinates and equivalent isotropic displacement parameters (\AA^2) for **1-2**. U(eq) is defined as one third of the trace of the orthogonalized U_{ij} tensor.

Complex 1	x	y	z	U(eq)
Ag1	0.07534 (2)	0.24016 (2)	0.93479 (3)	0.0330 (1)
C1	0.2964 (3)	0.0023 (2)	0.1763 (3)	0.0236 (7)
C2	0.3452 (3)	0.0166 (2)	0.0496 (3)	0.0298 (7)
C3	0.4792 (3)	-0.0071 (2)	0.0651 (3)	0.0313 (7)
C4	0.8988 (3)	0.1804 (2)	0.5836 (3)	0.0298 (7)
C5	0.8088 (3)	0.1731 (2)	0.6527 (3)	0.0287 (7)
C6	0.7576 (3)	0.2414 (2)	0.6959 (4)	0.0261 (7)
C7	0.8044 (3)	0.3146 (2)	0.6665 (4)	0.0319 (8)
C8	0.8944 (3)	0.3164 (2)	0.5972 (4)	0.0333 (8)
C9	0.6528 (3)	0.2366 (2)	0.7619 (4)	0.0303 (8)
C10	0.5258 (3)	0.2330 (2)	0.6465 (4)	0.0280 (7)
C11	0.4170 (3)	0.23506 (18)	0.7060 (3)	0.0236 (7)
C12	0.3885 (3)	0.3046 (2)	0.7710 (3)	0.0262 (7)
C13	0.2901 (3)	0.3044 (2)	0.8289 (3)	0.0267 (7)
C14	0.2440 (3)	0.17392 (2)	0.7658 (3)	0.0258 (7)
C15	0.3407 (3)	0.1695 (2)	0.7050 (3)	0.0239 (7)
N1	0.9421 (3)	0.2506 (1)	0.5522 (3)	0.0249 (6)
N2	0.2182 (3)	0.2403 (1)	0.8289 (3)	0.0236 (6)
O1	0.1797 (2)	0.0105 (1)	0.1579 (2)	0.0322 (5)
O2	0.3728 (2)	-0.0152 (1)	0.2940 (2)	0.0320 (5)
O1W	0.0468 (2)	0.0816 (1)	0.9042 (2)	0.0349 (6)
O2W	0.1654 (2)	-0.0058 (2)	0.6287 (3)	0.0433 (6)
O3W	0.0663 (2)	0.0680 (2)	0.3657 (3)	0.0420 (6)
O4W	0.6111 (2)	0.0448 (2)	0.4229 (2)	0.0423 (6)

Complex 2	x	y	z	U(eq)
Ag1	0.23392 (6)	0.60429 (3)	0.73725 (2)	0.0456 (2)
Ag2	0.5000	1.0000	0.5000	0.0488 (3)
Ag3	0.4894 (4)	0.50095 (16)	0.49110 (6)	0.0537 (7)
C1	0.4462 (9)	0.7045 (3)	0.6159 (2)	0.042 (2)

C2	0.466 (1)	0.7551 (4)	0.5923 (2)	0.057 (2)
C3	0.495 (1)	0.8013 (4)	0.6144 (2)	0.070 (3)
C4	0.644 (1)	0.8044 (4)	0.6356 (3)	0.067 (3)
C5	0.689 (1)	0.8528 (4)	0.6557 (3)	0.065 (3)
C6	0.7142 (9)	0.8998 (3)	0.6295 (2)	0.044 (2)
C21	0.3220 (9)	0.5897 (4)	0.5383 (2)	0.054 (2)
C22	0.2271 (8)	0.6307 (3)	0.5418 (2)	0.041 (2)
C23	0.1518 (7)	0.6503 (3)	0.5107 (2)	0.040 (2)
C24	0.1816 (9)	0.6243 (4)	0.4763 (2)	0.053 (2)
C25	0.274 (1)	0.5841 (5)	0.4750 (3)	0.068 (3)
C26	0.0540 (7)	0.6999 (3)	0.5130 (2)	0.0355 (16)
C27	0.1451 (7)	0.7496 (3)	0.5097 (2)	0.038 (2)
C28	0.0528 (7)	0.7998 (3)	0.5141 (2)	0.041 (2)
C29	0.2984 (9)	0.9162 (3)	0.5389 (2)	0.046 (2)
C30	0.2043 (8)	0.8740 (3)	0.5425 (2)	0.043 (2)
C31	0.1473 (7)	0.8487 (3)	0.5110 (2)	0.036 (2)
C32	0.1869 (8)	0.8703 (3)	0.4763 (2)	0.039 (2)
C33	0.2829 (8)	0.9129 (3)	0.4737 (2)	0.0407 (2)
C41	0.4514 (8)	0.5183 (3)	0.7125 (2)	0.043 (2)
C42	0.5488 (8)	0.4759 (4)	0.7145 (2)	0.045 (2)
C43	0.5903 (7)	0.4557 (3)	0.74995 (19)	0.040 (2)
C44	0.5299 (8)	0.4812 (3)	0.7819 (2)	0.042 (2)
C45	0.4358 (8)	0.5230 (3)	0.7775 (2)	0.042 (2)
C46	0.6885 (8)	0.4094 (3)	0.7537 (2)	0.041 (2)
C47	0.5992 (7)	0.3564 (3)	0.75044 (19)	0.033 (2)
C48	0.6982 (8)	0.3079 (3)	0.7544 (2)	0.036 (2)
C49	0.4580 (8)	0.1985 (3)	0.7126 (2)	0.043 (2)
C50	0.5479 (8)	0.2417 (3)	0.7156 (2)	0.038 (2)
C51	0.6060 (7)	0.2584 (3)	0.7507 (2)	0.034 (2)
C52	0.5695 (7)	0.2263 (3)	0.7815 (2)	0.041 (2)
C53	0.4767 (7)	0.1820 (4)	0.7766 (2)	0.045 (2)
N1	0.3925 (6)	0.5424 (3)	0.7435 (2)	0.039 (2)
N2	0.4212 (6)	0.1677 (2)	0.7429 (2)	0.036 (1)
N3	0.3482 (7)	0.5633 (3)	0.5060 (2)	0.055 (2)

N4	0.3394 (6)	0.9357 (3)	0.5050 (2)	0.042 (2)
O1	0.5609 (6)	0.6761 (3)	0.6185 (2)	0.070 (2)
O2	0.3227 (5)	0.6942 (2)	0.6297 (1)	0.043 (1)
O3	0.8444 (6)	0.9126 (2)	0.6223 (2)	0.053 (2)
O1W	0.2341 (5)	0.6014 (2)	0.6615 (1)	0.045 (1)
O2W	-0.0537 (6)	0.5955 (3)	0.6349 (2)	0.065 (2)
O3W	0.5091 (5)	1.0137 (2)	0.5835 (1)	0.053 (2)
O4W	0.2787 (5)	0.5113 (2)	0.6166 (2)	0.052 (2)
O5W	0.9382 (6)	1.0056 (3)	0.5922 (2)	0.066 (2)
O6W	0.6359 (7)	0.5815 (3)	0.6468 (2)	0.086 (2)
O7W	0.0753 (6)	0.7555 (3)	0.6151 (2)	0.076 (2)
O8W	0.3162 (6)	0.9139 (3)	0.6436 (2)	0.064 (2)
O9W	-0.1441 (6)	0.6851 (3)	0.60062 (17)	0.070 (2)
O10W	1.0761 (6)	0.8518 (2)	0.6514 (2)	0.060 (2)

Table S3. Selected bond distances (\AA) and angles ($^{\circ}$) for **1-2**.

Complex 1					
Ag1–N1 ⁱ	2.133(3)	Ag1–N2	2.139(3)	Ag1–O1w	2.681(2)
Ag1 ⁱⁱⁱ –N1	2.133(3)	C1–O1	1.268(4)	C1–O2	1.260(4)
C1–C2	1.517(4)	C2–C3	1.508(5)	C3–C3 ⁱⁱ	1.503(6)
N1 ⁱ –Ag1–N2	174.48(9)	N1 ⁱ –Ag1–O1w	93.15(8)	N2–Ag1–O1w	91.54(8)
Complex 2					
Ag1–N1	2.127(7)	Ag1–N2 ⁱ	2.133(6)	Ag1–O1w	2.659(5)
Ag2–N4	2.180(7)	Ag2–N4 ⁱⁱ	2.180(7)	Ag3–N3	2.089(8)
Ag3–N3 ⁱⁱⁱ	2.185(8)	C1–O1	1.259(9)	C1–O2	1.240(9)
C6–O3	1.241(9)	C6–O4	1.276(9)		
N1–Ag1–N2 ⁱ	168.7(2)	N1–Ag1–O1w	94.7(2)	N2 ⁱ –Ag1–O1w	96.6(2)
N4–Ag2–N4 ⁱⁱ	180.0(1)	N3–Ag3–N3 ⁱⁱⁱ	162.6(1)		

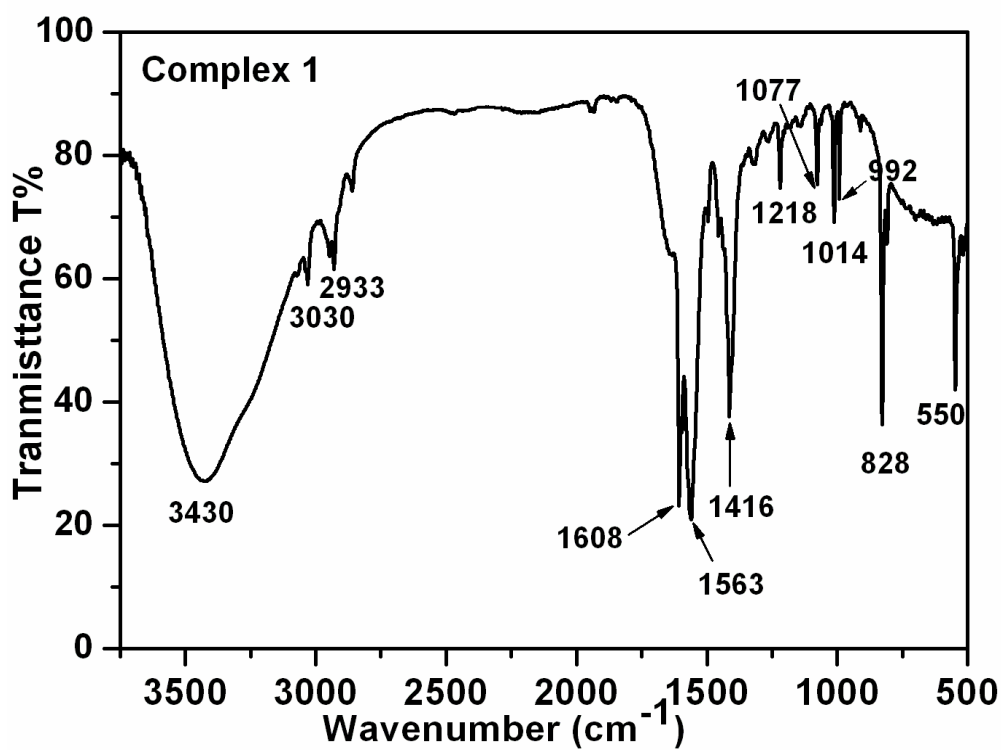
Symmetry codes: (i) $x-1, -y+1/2, z+1/2$; (ii) $-x+1, -y, -z$; (iii) $x+1, -y+1/2, z-1/2$ for **1**. (i) $-x+1/2, y+1/2, z$; (ii) $-x+1, -y+2, -z+1$; (iii) $-x+1, -y+1, -z+1$ for **2**.

Table S4. Relevant Hydrogen-bonding parameters in **1** and **2** (Å, °)^j.

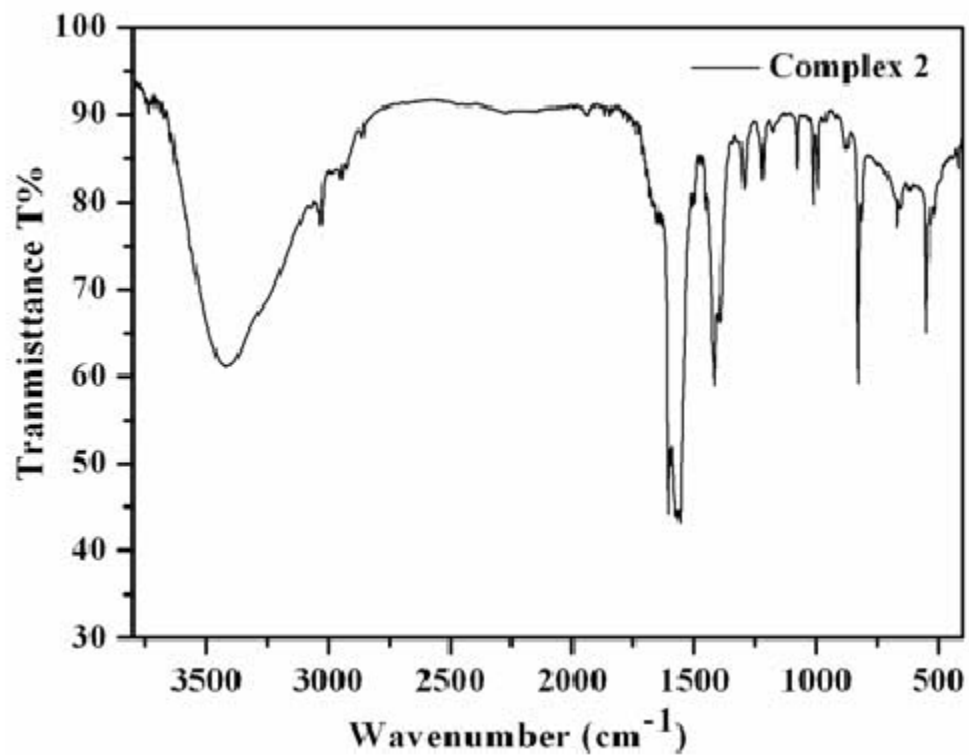
D–H···A	H···A	D···A	D–H···A	Symmetry equivalent operators
Complex 1				
O1w–H1wa···O1 ^{iv}	2.08	2.868(3)	169	-x, -y, -z+1
O1w–H1wb···O1 ^v	1.98	2.781(3)	178	x, y, z+1
O2w–H2wa···O4w ^{vi}	1.97	2.758(4)	168	-x+1, -y, -z+1
O2w–H2wb···O3w	2.00	2.797(4)	175	
O3w–H3wa···O1	2.07	2.864(3)	173	
O3w–H3wb···O2w ^{iv}	2.02	2.798(3)	164	-x, -y, -z+1
O4w–H4wa···O2 ^{vi}	2.01	2.790(3)	165	-x+1, -y, -z+1
O4w–H4wb···O2	2.05	2.779(3)	152	
Complex 2				
O1w–H1wa···O2	1.92	2.716(8)	175	
O1w–H1wb···O2w	1.96	2.757(7)	175	
O2w–H2wa···O3w ^{iv}	1.98	2.772(8)	173	-x+1/2, y-1/2,z
O2w–H2wb···O6w ^v	2.06	2.845(8)	167	
O3w–H3wa···O4	1.89	2.680(8)	170	
O3w–H3wb···O4w ⁱ	2.29	2.839(7)	127	-x+1/2, y+1/2, z
O4w–H4wa···O1w	2.36	2.797(8)	116	
O4w–H4wb···O8w ^{iv}	1.98	2.770(9)	172	-x+1/2, y-1/2,z
O5w–H5wa···O4w ^{vi}	1.89	2.692(7)	176	-x+3/2, y+1/2, z
O5w–H5wb···O3	1.91	2.710(8)	176	
O6w–H6wa···O5w ^{vii}	1.99	2.791(9)	179	-x+3/2, y-1/2, z
O6w–H6wb···O1	1.87	2.674(9)	179	
O7w–H7wa···O9w	2.04	2.705(9)	140	
O7w–H7wb···O2	1.96	2.759(8)	177	
O8w–H8wa···O10w ^v	1.95	2.684(8)	153	x-1, y, z
O8w–H8wb···O4	1.98	2.719(7)	153	
O9w–H9wa···O1 ^v	1.94	2.737(8)	172	x-1, y, z
O9w–H9wb···O2w	2.05	2.687(9)	137	
O10w–H10b···O3	1.98	2.782(8)	180	

Fig. S1. FT-IR spectra of **1-2**.

(a)



(b)



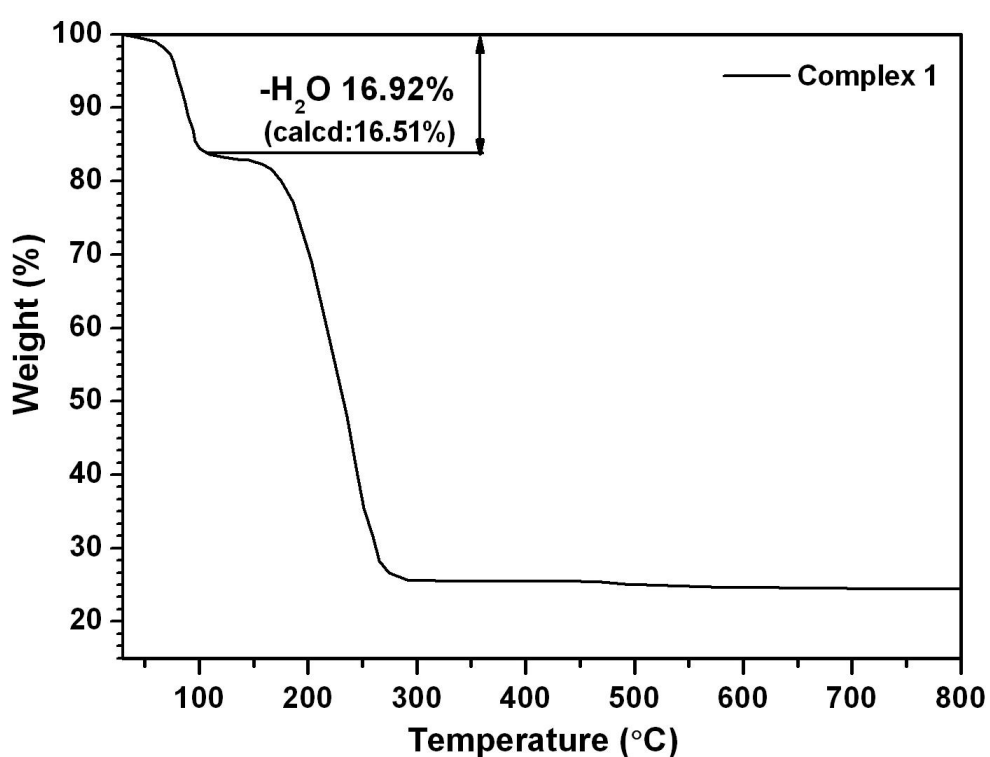
Comment on IR spectra

The solid-state IR spectra of **1** and **2** are quite similar and exhibit characteristic bands of adip²⁻, bpp, and bpe ligands in the region 4000-400 cm^{-1} . The O-H stretching frequency of the water cluster is observed at

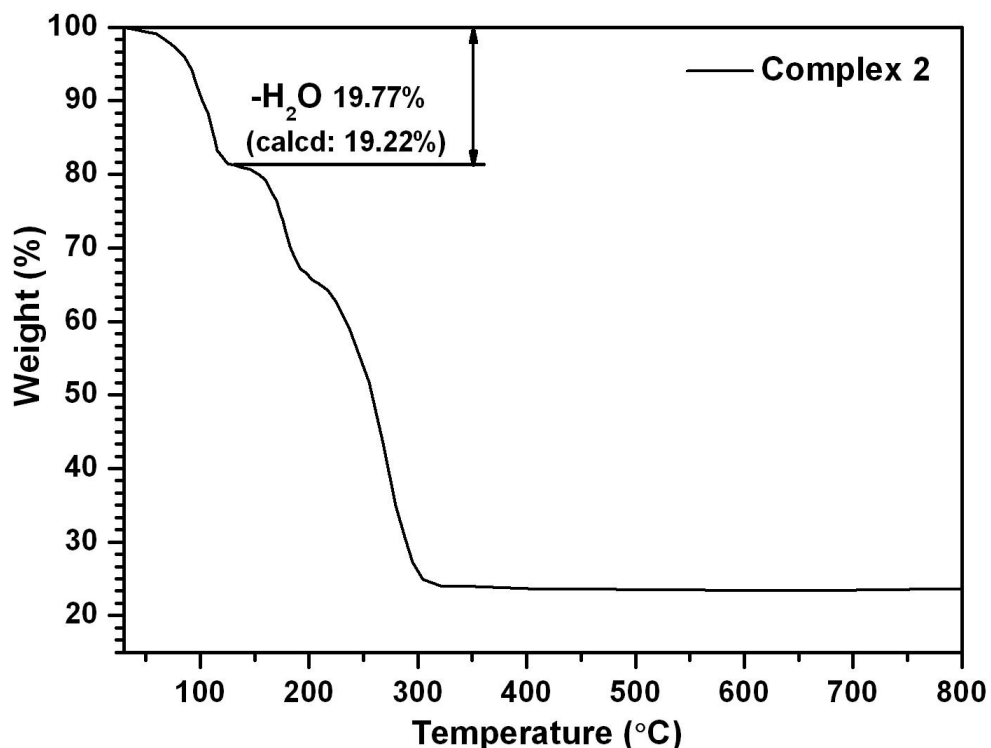
about 3430 cm^{-1} for **1** (3460 cm^{-1} for **2**). Generally, the IR spectrum of ice shows the O-H stretching band at 3220 cm^{-1} , while this stretching vibration in liquid water appears at 3490 cm^{-1} . This suggests that the water clusters in **1-2** show O-H stretching vibrations similar to that of liquid water, and the slight difference is attributable to the environment that the clusters are in. The peaks around 1608 , 1563 and 1416 cm^{-1} for **1** (1612 , 1558 and 1420 cm^{-1} for **2**) can be attributed to the asymmetric and symmetric vibrations of the carboxylate groups. There are no bands in the region 1690 - 1730 cm^{-1} , indicating complete deprotonation of the H₂suc molecules. These are consistent with the results of the X-ray diffraction analysis.

Fig. S2. TGA curves of **1-2**.

(a)



(b)

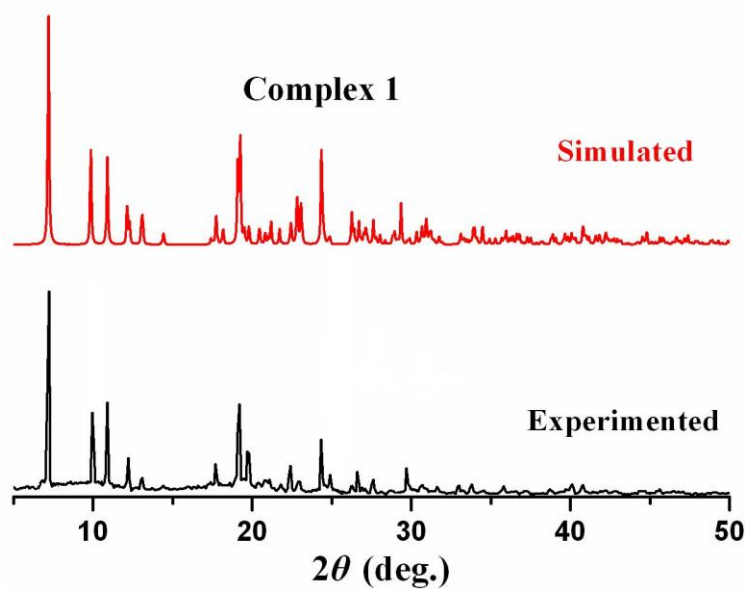


Comment on TGA

Thermogravimetric (TG) analysis has been performed on single-phase polycrystalline samples of **1** and **2** between 25 and 800 °C. The results indicate that **1** showed an initial weight loss of 16.92% from ~25 to ~105 °C corresponding to the removal of eight water molecules per formula unit (calcd: 16.51%), and then the framework starts to decompose accompanying loss of organic ligands. For **2**, the TG curve is similar to that of **1**: the weight loss of 19.77% below ~110 °C (calcd: 19.22%) is attributed to loss of ten lattice water molecules, and then the framework of **2** begins to collapse in the temperature range 110–300 °C, which indicates the contribution of the water cluster to the stability of the crystal host and is similar to complex **1** and some reported species.

Fig. S3: Powder XRD patterns and simulated one from the single-crystal diffraction data for **1** (a) and **2** (b).

(a)



(b)

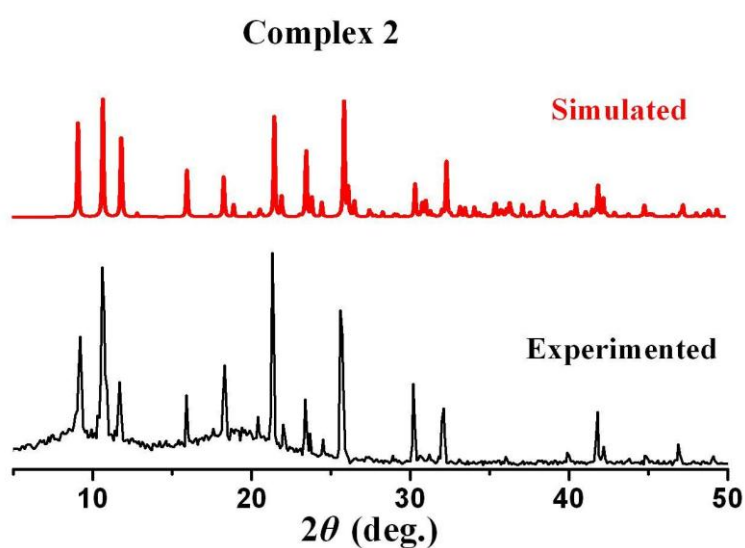
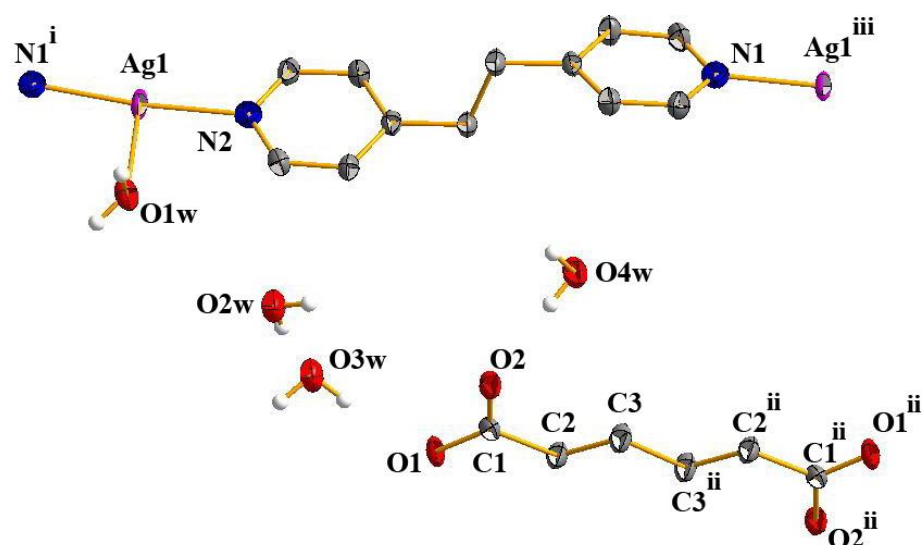


Fig. S4. ORTEP diagrams showing the building units of crystal structures in **1-2** (50% thermal probability ellipsoids). The hydrogen atoms at either aromatic ring or methylene are omitted for clarity. Symmetry codes: (i) $x-1, -y+1/2, z+1/2$; (ii) $-x+1, -y, -z$; (iii) $x+1, -y+1/2, z-1/2$, for **1**. (i) $-x+1/2, y+1/2, z$; (ii) $-x+1, -y+2, -z+1$; (iii) $-x+1, -y+1, -z+1$; (iv) $-x+1/2, y-1/2, z$, for **2**.

(a)



(b)

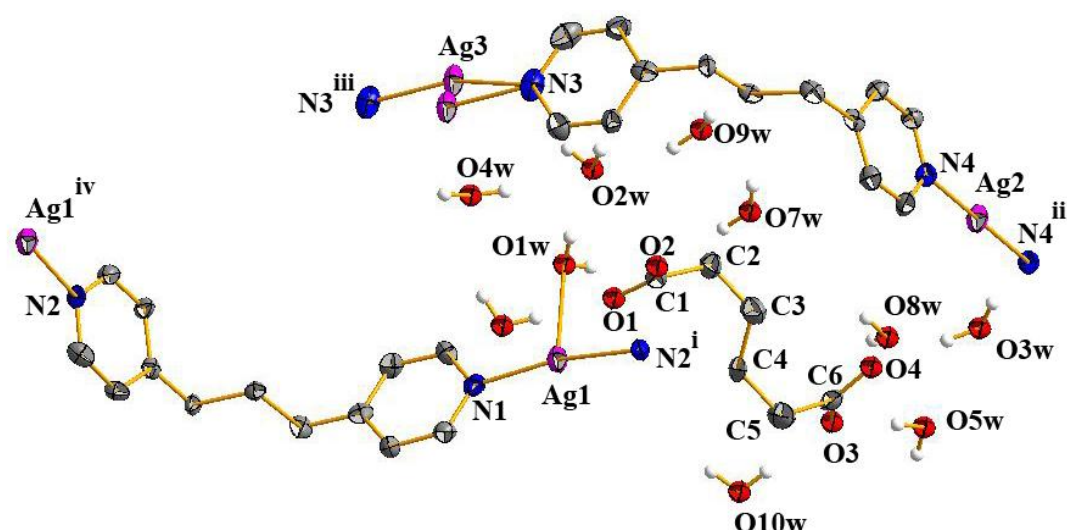


Fig. S5. 2D water-adip anionic layer formed by hydrogen-bonding in **1**.

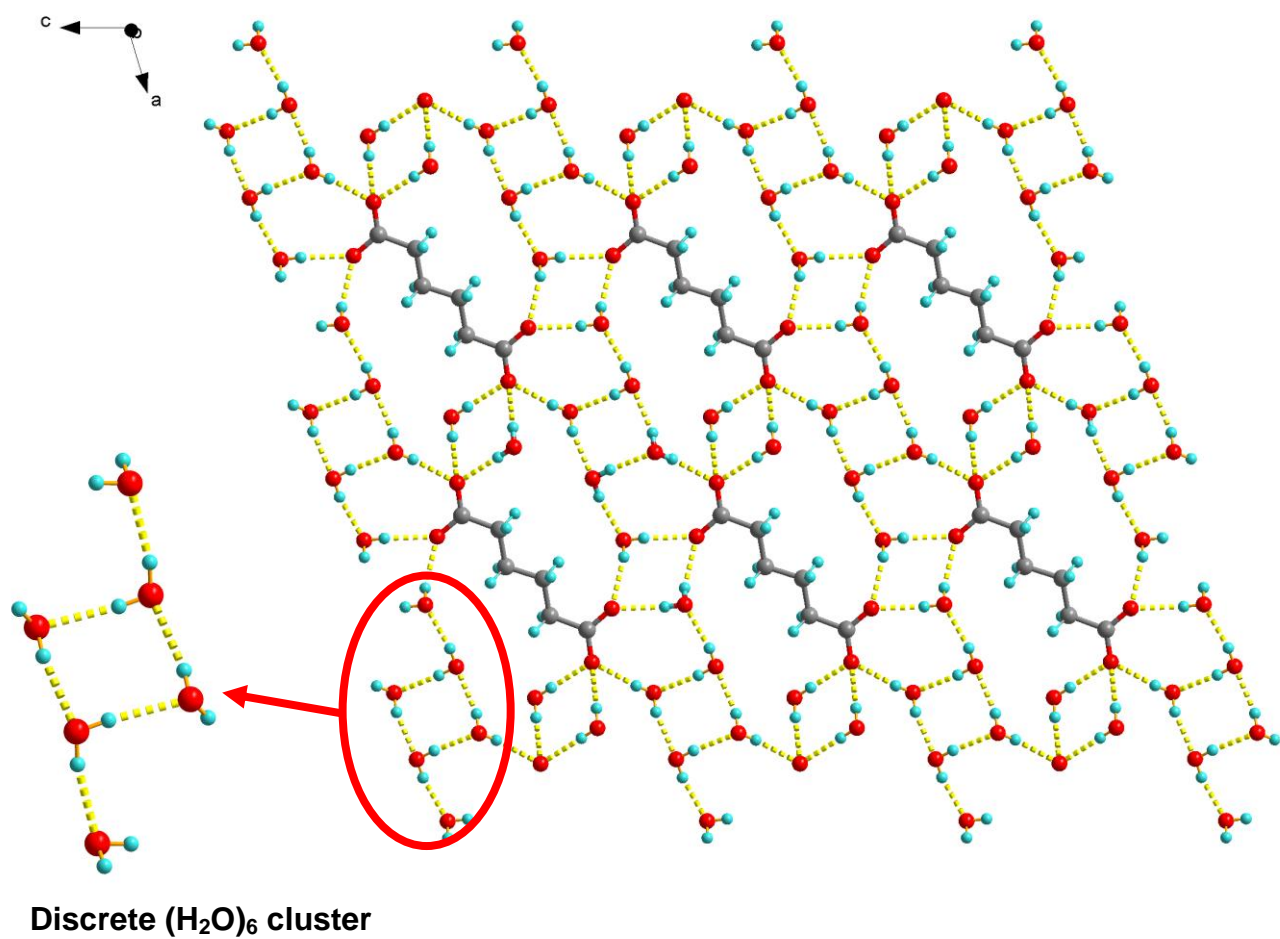
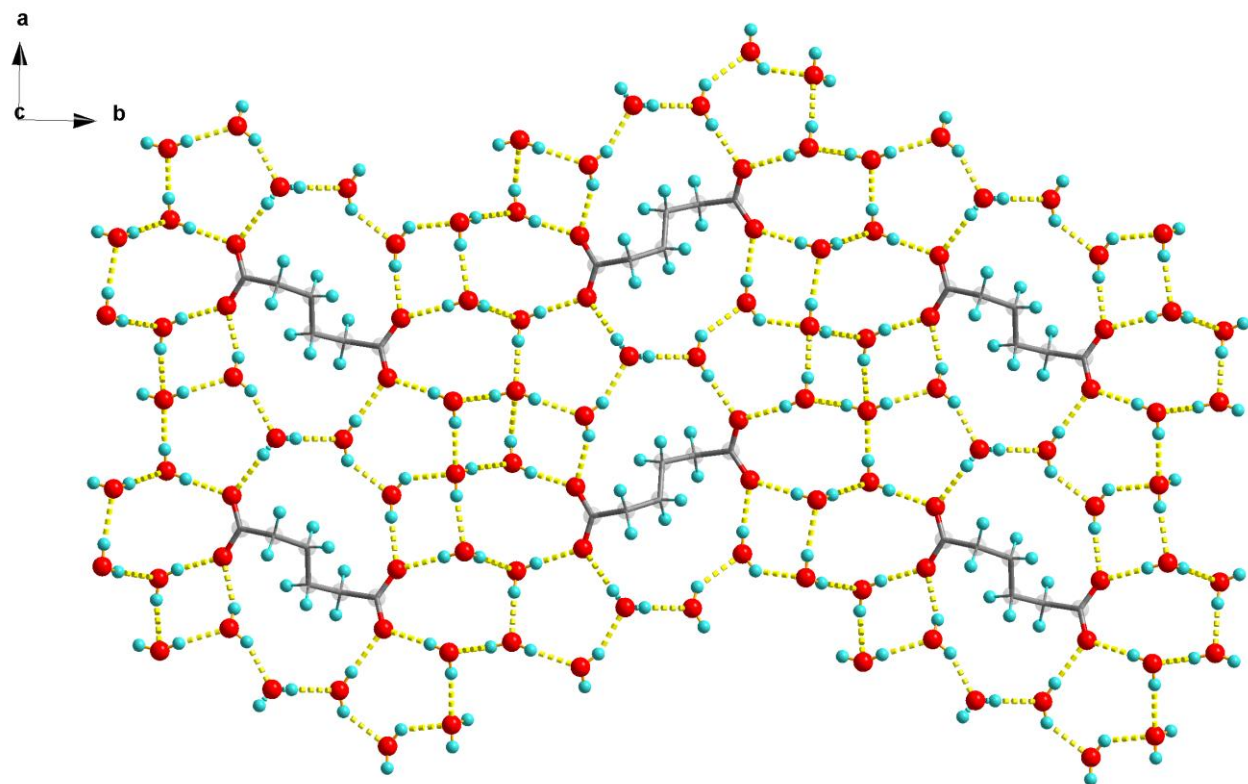


Fig. S6. (a) 2D water-adip anionic layer formed by hydrogen-bonding in **2**. (b) Perspective view of L4(4)20(16) water layer along the *c*-axis; adipate dianions are omitted for clarity.

(a)



(b)

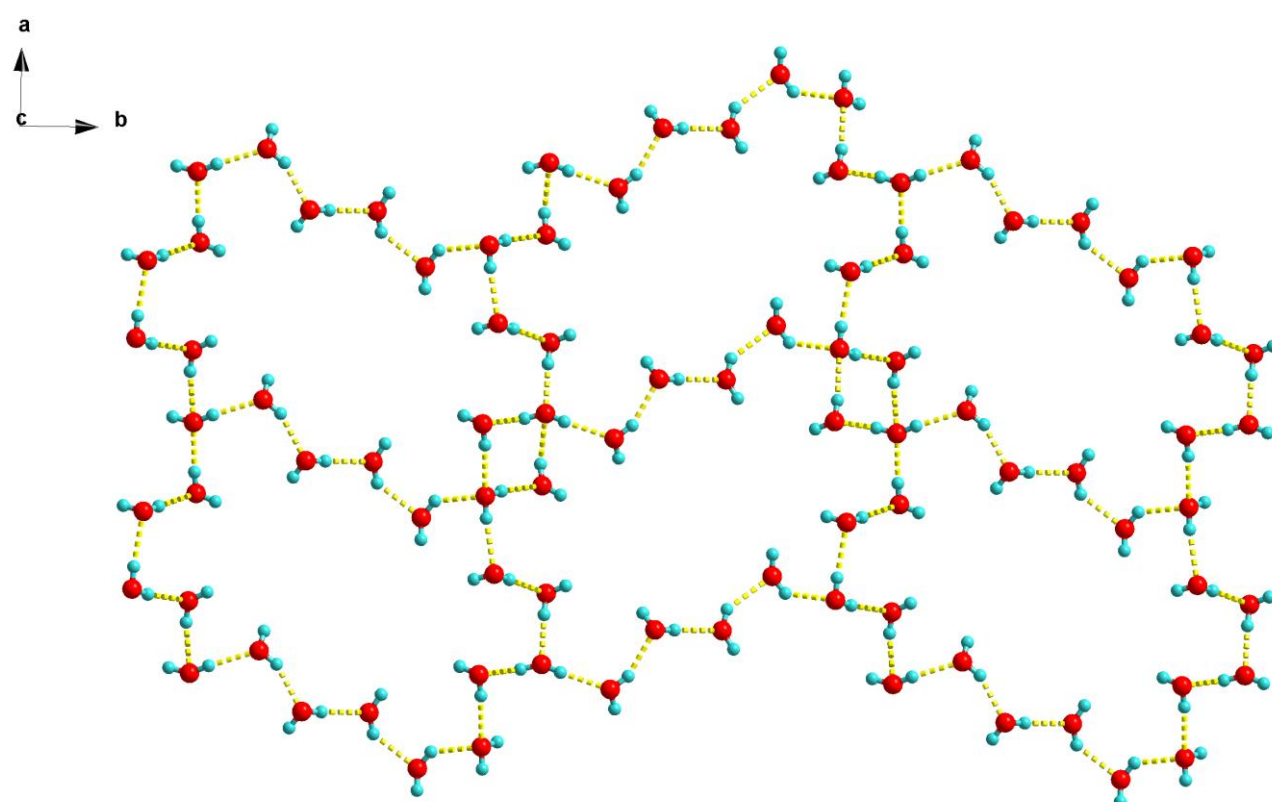
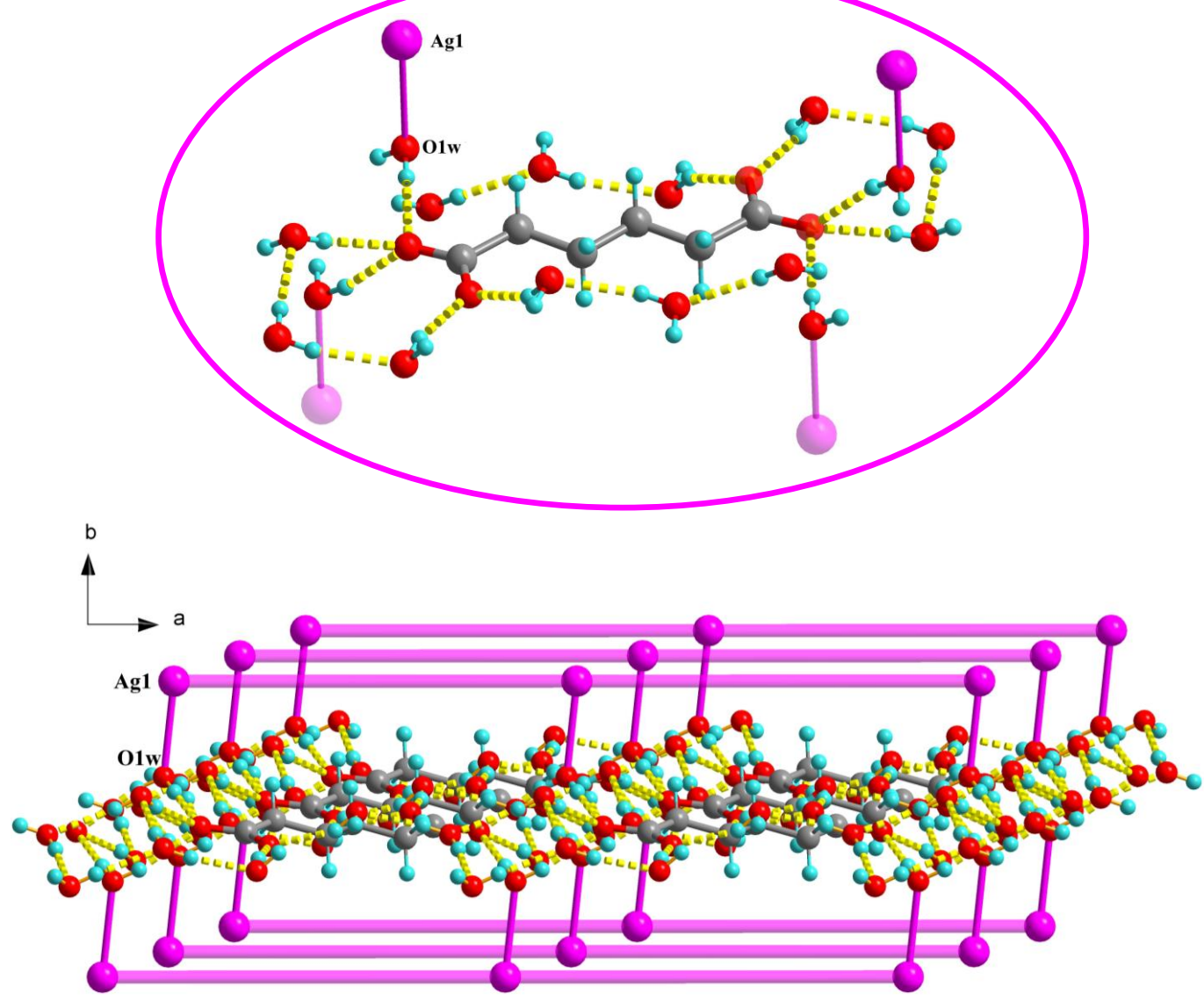
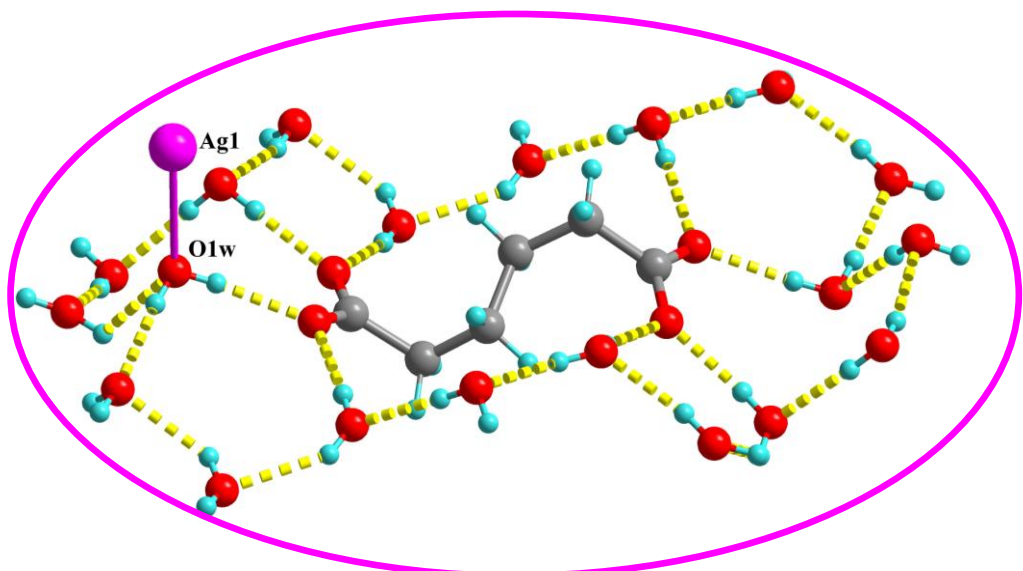


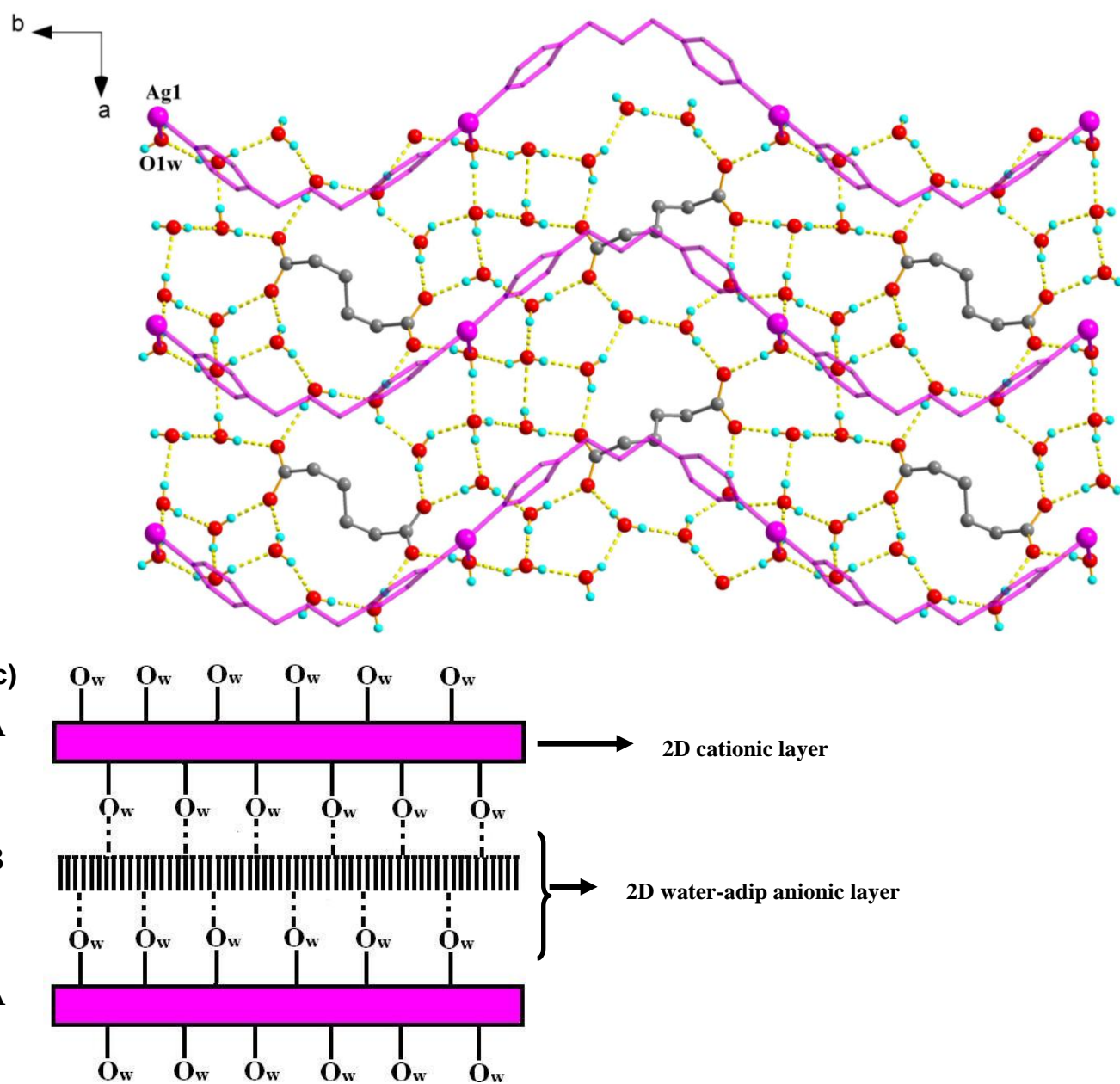
Fig. S7. Metallo-supramolecular sandwich lamellar networks occurred in **1** (a) and **2**(b); (c) A schematic representation of the H-bonding stacking arrays in **1** and **2**.

(a)



(b)





Comments

As shown in Figure S7a-b, in the $\{[(\text{adip}) \cdot 6\text{H}_2\text{O}]^{2-}\}_n$ anionic layer of **1**, the $(\text{adip})_{aaa} \cdot (\text{H}_2\text{O})_{16}$ anionic clusters [or $(\text{adip})_{gag} \cdot (\text{H}_2\text{O})_{20}$ from the $\{[(\text{adip}) \cdot 9\text{H}_2\text{O}]^{2-}\}_n$ anionic layer for **2**] are linked by water molecules O_w (recall that this O_w is a weak coordination member of the cationic host polymer $\{[\text{Ag}_2(\text{bpe})_2(\text{H}_2\text{O})_2]^{2+}\}_n$ for **1** ($\text{Ag1-O1w} = 2.681(2)$ Å) or $\{[\text{Ag}_2(\text{bpp})_2(\text{H}_2\text{O})]^{2+}\}_n$ for **2** ($\text{Ag1-O1w} = 2.659(5)$ Å)), so it appears to be important for stabilization of the whole guest anionic layer), to give a metallo-supramolecular sandwich lamellar network along $\sim[001]$ direction following the alternating -ABAB- sequence, in which those water-anion layered species are occupied in the interlayer spacing between metallo-organic networks (Figure S7c).